The EMBO Journal Vol.17 No.16 pp.4723–4734, 1998

Constitutive activation of delayed-rectifier potassium channels by a Src family tyrosine kinase in Schwann cells

Alexander Sobko, Asher Peretz and Bernard Attali[1]

Neurobiology Department, Weizmann Institute of Science, Rehovot 76100, Israel

[1]Corresponding author
e-mail: bnattali@weizmann.weizmann.ac.il

A.Sobko and A.Peretz contributed equally to this work

In the nervous system, Src family tyrosine kinases are thought to be involved in cell growth, migration, differentiation, apoptosis, as well as in myelination and synaptic plasticity. Emerging evidence indicates that K^+ channels are crucial targets of Src tyrosine kinases. However, most of the data accumulated so far refer to heterologous expression, and native K^+-channel substrates of Src or Fyn in neurons and glia remain to be elucidated. The present study shows that a Src family tyrosine kinase constitutively activates delayed-rectifier K^+ channels (I_K) in mouse Schwann cells (SCs). I_K currents are markedly downregulated upon exposure of cells to the tyrosine kinase inhibitors herbimycin A and genistein, while a potent upregulation of I_K is observed when recombinant Fyn kinase is introduced through the patch pipette. The Kv1.5 and Kv2.1 K^+-channel α subunits are constitutively tyrosine phosphorylated and physically associate with Fyn both in cultured SCs and in the sciatic nerve *in vivo*. Kv2.1- channel subunits are found to interact with the Fyn SH2 domain. Inhibition of Schwann cell proliferation by herbimycin A and by K^+-channel blockers suggests that the functional linkage between Src tyrosine kinases and I_K channels could be important for Schwann cell proliferation and the onset of myelination.

Keywords: K^+ channels/myelination/proliferation/Schwann cell/Src kinase

Introduction

The non-receptor protein tyrosine kinases of the Src family are key components of signal transduction pathways for a wide range of cellular processes, including gene transcription, cell growth, migration, differentiation, apoptosis as well as synaptic plasticity and ionic channel modulation (Bolen, 1993; Courtneidge, 1994; Erpel and Courtneidge, 1995; Jonas and Kaczmarek, 1996; Thomas and Brugge, 1997; Boxall and Lancaster, 1998). Consistent with their crucial role in neuronal functions, Src family tyrosine kinases such as Fyn, Yes and Src are highly expressed in neurons and glia. The expression of Fyn and Src is widespread in the brain, especially in the hippocampus (Ross *et al*., 1988; Umemori *et al*., 1992). Disruption of the Fyn gene is associated with architectural abnormalities in the hippocampus, defects in long term potentiation and spatial learning (Grant *et al*., 1992). Interestingly, Fyn is also expressed in oligodendrocytes where it interacts with myelin-associated glycoprotein (MAG) and Fyn-mutant mice show reduced CNS myelination, probably due to disruption of MAG signaling (Umemori *et al*., 1994). Likewise, Fyn is abundantly expressed in Schwann cells (SCs), the myelin-forming cells of the peripheral nervous system (Bare *et al*., 1993).

Emerging evidence indicates that various voltage-dependent and ligand-gated ionic channels are crucial targets of Src tyrosine kinases (Jonas and Kaczmarek, 1996; Thomas and Brugge, 1997; Boxall and Lancaster, 1998). Fyn and Src kinases can phosphorylate the δ and β subunits of the nicotinic acetylcholine receptor in *Torpedo* electric organ and C2 cultured myotubes, respectively, and this process is suggested to play a role in receptor clustering (Swope and Huganir, 1994; Fuhrer *et al*., 1997). The NR2A subunit of NMDA receptors is also found to be a target of Src and Fyn upon heterologous expression in HEK 293 cells, while in dorsal horn spinal neurons Src upregulates *N*-Methyl-D-Aspartate (NMDA) receptor currents by increasing the channel open probability (Kohr and Seeburg, 1996; X.-M.,Yu *et al*., 1997). Src tyrosine kinases can also regulate the activity of voltage-gated K^+ channels (Kv). In the Jurkat T cell line, the $p56^{lck}$-mediated phosphorylation of the Kv1.3 K^+-channel subunit correlates with an inhibition of voltage-sensitive K^+ currents upon Fas stimulation which is suggested to be relevant for apoptosis (Szabo *et al*., 1996). Similarly, coexpression of Kv1.3 K^+ channel with constitutively active v-Src in HEK 293 cells leads to a decrease in K^+-current amplitude and a slowing of C-type inactivation as well as an increased tyrosine phosphorylation of the K^+-channel protein (Holmes *et al*., 1996a; Fadool *et al*., 1997). The human Kv1.5 K^+ channel can associate via its N-terminus-located proline-rich sequence with the SH3 domain of the Src kinase upon coexpression in HEK 293 cells and in human cardiac ventricular membranes (Holmes *et al*., 1996b). Coexpression of Kv1.5 with v-Src leads to tyrosine phosphorylation of the channel and to a decrease in its activity; however, it remains to determine whether this process occurs *in vivo* under physiological conditions (Holmes *et al*., 1996b).

In spite of these various studies, yet little is known about the functional signaling of Src tyrosine kinases in central and peripheral neurons as well as in glial cells. As far as K^+ channels are concerned, most of the data obtained so far relate to heterologously expressed proteins, and native substrates of Src or Fyn in neurons and glia remain to be elucidated. Given the importance of K^+ channels and Src family tyrosine kinases for the development, proliferation and differentiation of glial cells (Trotter *et al*.,

1989; Barres *et al*., 1990; Chiu, 1991; Ritchie, 1992; Bare *et al*., 1993; Sontheimer, 1994, 1995; Attali *et al*., 1997), we set out to determine whether K^+ channels could be subject to regulation by Fyn tyrosine kinase in mouse primary cultured SCs and in the sciatic nerve. Results of the present study indicate that the Src family tyrosine kinase constitutively activates delayed-rectifier K^+ channels (I_K) and that this functional linkage may be important for SC mitogenesis and differentiation.

Results

Proliferating Schwann cells actively express Kv channels

SCs were purified from P4 mouse sciatic nerves, at a time when they are known to proliferate, exhibiting mostly a premyelinating phenotype (Mirsky and Jessen, 1996; Zorick and Lemke, 1996). Cells were grown *in vitro* for 2–7 days in the presence of serum; under these conditions, they actively proliferated and expressed the SC marker S-100, a Ca^{2+}-binding protein (Figure 1B, B1 and B2). Macroscopic currents were recorded from cultured SCs using the whole-cell configuration of the patch–clamp technique (Hamill *et al*., 1981). All SCs exhibited prominent voltage-gated outward K^+ currents which activated upon membrane depolarization (Figure 2). In agreement with previous studies (Hoppe *et al*., 1989; Konishi, 1989; Amedee *et al*., 1991; Wilson and Chiu, 1993), the whole-cell recordings clearly identified the presence of a transient and a sustained K^+ current components (Figure 2A). The normalized conductance curves of activation fitted to a single Boltzmann distribution (Figure 2B, left panel) and showed that there was no noticeable difference between the two kinetic components. The K^+ currents were activated above a threshold of approximately –50 mV with $V_{50} = –16.5 \pm 0.9$ mV and $V_{50} = –18.1 \pm 0.9$ mV, slopes $s = –9.7 \pm 0.5$ and $s = –8.9 \pm 0.5$ for the transient and the sustained components, respectively ($n = 28$; ± SEM). The Boltzmann-fitted steady-state inactivation curves (Figure 2B, right panel) indicated that the transient component inactivated at more hyperpolarized potentials (by –8.8 mV), relative to the sustained component with $V_{50} = –18.3 \pm 2.2$ mV and $V_{50} = –9.5 \pm 0.5$ mV, slopes $s = 16.8 \pm 0.7$ and $s = 17.2 \pm 0.6$, respectively ($n = 4$). However, we were unable to separate the two kinetic components. As far as the pharmacology is concerned, the voltage-gated K^+ currents in SCs were highly sensitive to block by 50 μM quinidine (~80% inhibition) and were moderately affected by 1 mM 4-aminopyridine (4-AP; ~20% inhibition) (Figure 2A, lower trace and data not shown, respectively).

We characterized the expression of individual Kv-channel α subunits in cultured SCs, using RT–PCR cloning and a battery of subunit-specific polyclonal and monoclonal antibodies (Sobko,A., Peretz,A., Shirihai,O., Etkin,S., Cherepanova,V., Dagan,D. and Attali,B., in preparation). The specificity of antibody staining in SCs was checked by preabsorbing the antisera with their respective antigens and by analyzing the labeling pattern in transfected cells (data not shown), as previously described (Attali *et al*., 1997). Immunoblot and immunoprecipitation analyses indicated that Kv1.5, Kv2.1 and Kv3.1b α subunits of the mammalian *Shaker*, *Shab* and *Shaw* subfamilies, respectively, were abundantly expressed in SCs. For Kv1.5, two specific immunoreactive bands were observed, a major 65 kDa and an additional 90 kDa species. The 90 kDa species has been previously described in rat SCs (Mi *et al*., 1995) and possibly reflects post-

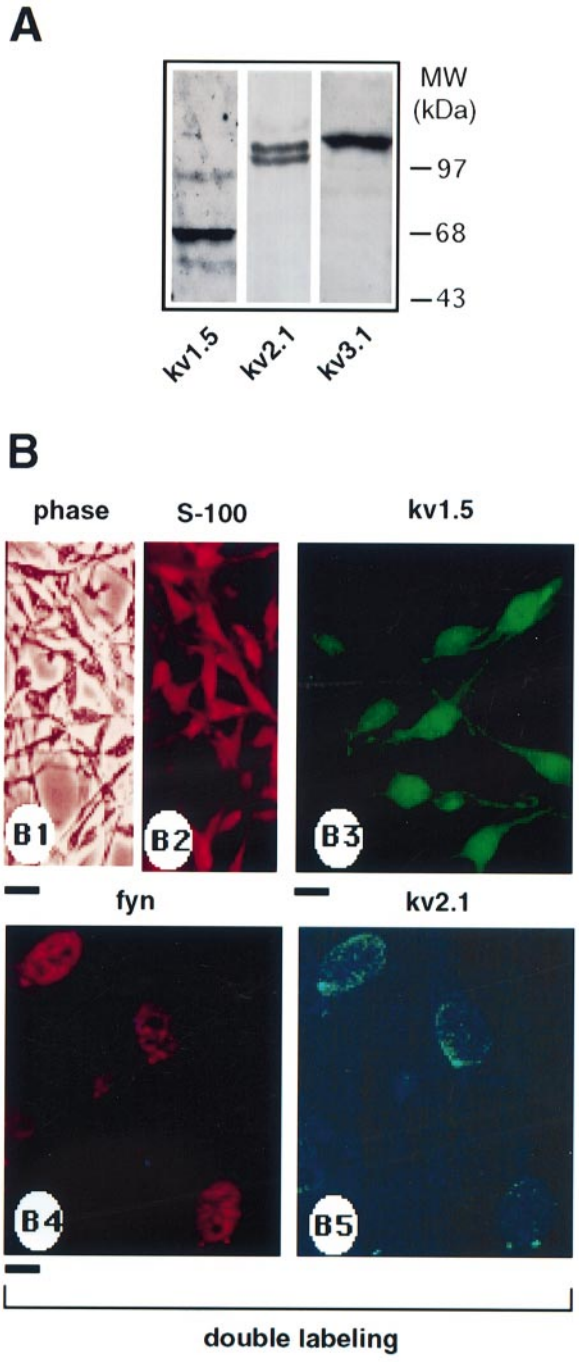

Fig. 1. Immunoblot and immunofluorescence analyses of Schwann cell cultures with antibodies to Kv-channel α subunits. (**A**) Membrane fractions of mouse primary cultured SCs were subjected to immunoblot analysis with subunit-specific antibodies to Kv1.5, Kv2.1 and Kv3.1b α subunits. HRP-conjugated secondary antibodies and ECL were used for detection. (**B**) Cells were labeled with anti-S-100 antibodies to confirm SC identity (B1 and B2). Staining with anti-kv1.5 is shown (B3). SCs were double-labeled with mouse monoclonal anti-fyn (B4) and rabbit polyclonal anti-kv2.1 (B5). Indirect immunofluorescence with anti-rabbit FITC and anti-mouse TRITC was used for detection. In B1–B2, B3 and B4–B5, the scale bar is 27 μM, 10 μM and 6.5 μM, respectively.

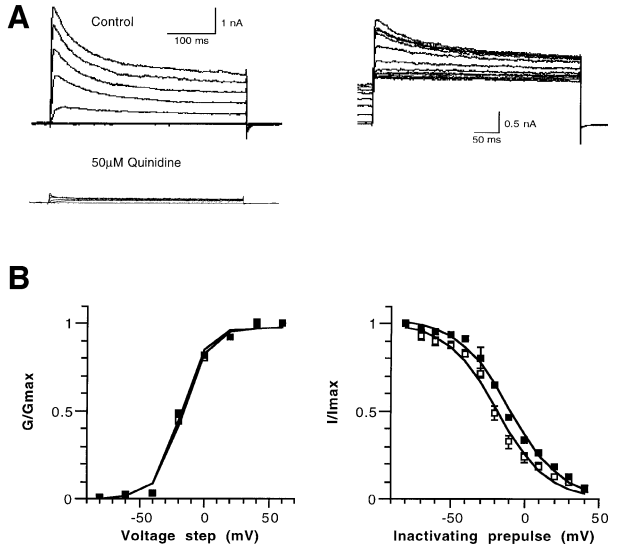

Fig. 2. Voltage-gated potassium currents in Schwann cells. (**A**) Whole-cell currents were recorded from voltage-clamped SCs that were held at –80 mV and stepped to +60 mV in 20 mV increments for 400 ms pulse duration (left panel). The currents showed transient and sustained components. The lower trace shows the potent block of the currents by 50 μM quinidine. In the steady-state inactivation protocol, cells were subjected to 1 sec inactivating prepulse from –80 mV to +10 mV in 10 mV increments and stepped to +60 mV test pulse of 400 ms duration (right panel). (**B**) Steady-state activation curves generated by the activation protocol as in (A). The normalized conductances (G/G_{max}) of the transient (□) and sustained (■) components were plotted against the voltage step and were fitted to a single Boltzmann distribution (left panel). Note that the error bars are smaller than the symbols. Steady-state inactivation curves were generated by the inactivation protocol as in (A). The normalized current amplitudes (I/I_{max}) of the transient (□) and sustained (■) components were plotted against the voltage step and were fitted to single Boltzmann distributions (right panel). The data shown are expressed as mean ± SEM (n = 28 and n = 4 for steady-state activation and inactivation curves, respectively).

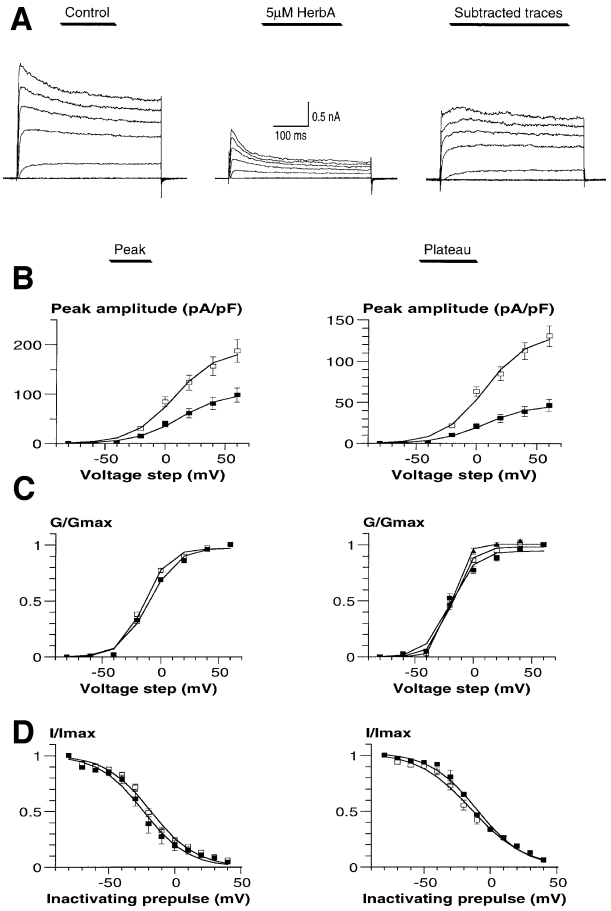

Fig. 3. Herbimycin A-induced downregulation of the K^+ currents. (**A**) Cultured SCs were stepped for 400 ms from a holding potential of –80 mV to +60 mV in 20 mV increments, before (left) and after (middle) 15 min application of 5 μM herbimycin A (Herb A). Subtracted traces are shown (right). For (B), (C) and (D), the left and right panels refer to the transient (peak) and sustained (plateau) components, respectively. (**B**) The whole-cell normalized current amplitudes (pA/pF) were plotted against the voltage steps (mV), in absence (□) and presence (■) of Herb A. The curves were fitted to single Boltzmann distributions. (**C**) The steady-state activation curves before (□) and after (■) Herb A exposure were constructed from (B) and fitted to single Boltzmann distributions. The normalized conductance curve of activation corresponding to the subtracted traces is also shown (▲, right panel). The error bars are smaller than the symbols. (**D**) Respective steady-state inactivation curves. The data shown are means ± SEM; n = 15. For the detailed Boltzmann fitting parameters, see Table I.

translational modifications. Occasionally, a lower band of ~47 kDa was detected; this band is not specific, since it is not blocked following preadsorption with the Kv1.5 antigen (not shown). For Kv2.1 a specific doublet of ~105 and 115 kDa immunoreactive bands was detected while for Kv3.1b a single specific 126 kDa species was observed (see Figures 1A, 6 and 7). These values are close to those previously described either in neurons, glia or transfected cells (Maletic-Savatic *et al*., 1995; Mi *et al*., 1995; Bekele-Arcuri *et al*., 1996; Attali *et al*., 1997), except for Kv3.1b isoform whose molecular weight is slightly higher in SCs, possibly due to a different post-translational processing (Du *et al*., 1996). Immunofluorescence staining with anti-Kv2.1 antibodies demonstrated moderate but consistent labeling of SC membranes, mainly around the cell soma with cluster-like patterns, while anti-Kv1.5 antibodies revealed that nearly all SCs somata and processes were stained more or less uniformly (Figure 1B).

Constitutive activation of voltage-dependent K^+ currents by Src family tyrosine kinase: effect of herbimycin A, genistein and recombinant Fyn $p55^{fyn}$

Cultured SCs were treated with the potent membrane permeable tyrosine kinase inhibitor, herbimycin A (Uehara and Fukazawa, 1991). Current amplitudes were measured in the same cell at the peak and plateau (end of depolarizing pulse) of the traces, before and after herbimycin A application. Following a 15 min exposure to 5 μM herbimycin A (Figure 3A and B), the maximal K^+-current amplitude was inhibited by 46% for the transient component (I_{max}= 189.6 ± 28.0 pA/pF reduced to 103.2 ± 15.6 pA/pF, n = 15) and by 65% for the sustained component (I_{max}= 130.5 ± 21.1 pA/pF reduced to 46.1 ± 7.2 pA/pF, n = 15). The normalized conductance and steady-state inactivation curves (Figure 3C and D) did not show significant changes in the voltage dependence of activation and inactivation gating in response to herbimycin A (Table I). The herbimycin action occurred within the 0.5–5 μM concentration range, initiated at ~5 min, reached steady-state within 15 min and was barely washed out (data not shown). Interestingly, analysis of the

Table I. Effect of herbimycin A on the activation and steady-state inactivation parameters

	Normalized I–V I_{max} (pA/pF)	Activation		Steady-state inactivation	
		V_{50} (mV)	slope (mV/e fold)	V_{50} (mV)	slope (mV/e fold)
Transient component (peak)					
Control	189.6 ± 28.0	–14.2 ± 1.0	–9.6 ± 0.5	–18.3 ± 2.2	16.8 ± 0.7
Herbimycin A	103.2 ± 15.6	–10.1 ± 1.5	–11.6 ± 0.6	–22.8 ± 4.9	15.1 ± 0.8
Sustained component (plateau)					
Control	130.5 ± 12.2	–18.0 ± 1.3	–7.7 ± 0.7	–9.4 ± 0.5	17.1 ± 0.6
Herbimycin A	46.1 ± 7.2	–17.8 ± 2.1	–10.4 ± 1.5	–14.8 ± 3.6	20.1 ± 1.8

All parameters were fitted to single Boltzmann distributions and the data are expressed as mean ± SEM of $n = 15$ experiments. Herbimycin A was used at 5 μM. The transient and sustained current amplitudes were measured at the peak and at the end (400 ms) of the depolarizing traces, respectively.

subtracted traces indicated that the main component affected by herbimycin A treatment corresponded to a slowly inactivating delayed-rectifier K^+ current (Figure 3A), whose normalized conductance curve overlapped with that of the control K^+ currents (Figure 3C, right panel). Similar results were obtained when another tyrosine kinase inhibitor, genistein, was used. Following a 10 min exposure to 100 μM genistein, the maximal K^+-current amplitude was inhibited by 56% for the transient component (I_{max}= 397 ± 47 pA/pF reduced to I_{max}= 174 ± 19 pA/pF, $n = 12$) and by 70% for the sustained component (I_{max}= 241 ± 24 pA/pF reduced to I_{max}= 74 ± 17 pA/pF, $n = 12$). Daizdein (100 μM), the structurally-related but inactive analog of genistein was totally ineffective, even after 20 min incubation ($n = 5$; not shown), clearly revealing the specificity of the genistein inhibitory action. To test more directly whether Src tyrosine kinases could regulate voltage-gated K^+ channels in SCs, recombinant p55-fyn was applied intracellularly through the patch pipette. Thus, when purified p55-fyn protein kinase (30 U/ml) and ATP (5 mM) were introduced into the patch-recording pipette, the whole-cell K^+-current amplitude increased by >60% (Figure 4C). Representative recordings (Figure 4A) from the same cell, 1 min (left panel) and 6 min (middle panel) after establishing the whole-cell configuration with their corresponding I–V relationships (Figure 4B), illustrated the upregulating effect of the Fyn kinase. The onset of Fyn kinase action was at ~3 min and it reached steady-state at 5–6 min. Herbimycin A (5 μM) included into the patch pipette, prevented the Fyn kinase upregulation and depressed the actual K^+-current amplitude (data not shown). When either ATP or the Fyn kinase alone was introduced into the patch-recording pipette, no effect was observed on the K^+ currents. Likewise, neither heat-inactivated Fyn kinase nor bovine serum albumin (into the patch pipette) produced any effects on the recorded K^+ currents (data not shown). As for herbimycin A data, analysis of the subtracted traces indicated that the K^+ current induced by recombinant p55-fyn tyrosine kinase treatment mainly corresponded to a slowly inactivating delayed-rectifier (Figure 4A, right panel). The increasing contribution of the delayed-rectifier K^+ current led to an enhancement of the sustained component (plateau) and an apparent upregulation of the peak current amplitude (Figure 4B and C). Consequently, there was an overall change in the whole-cell K^+-current inactivation kinetics (Figure 5). The control traces were best fitted

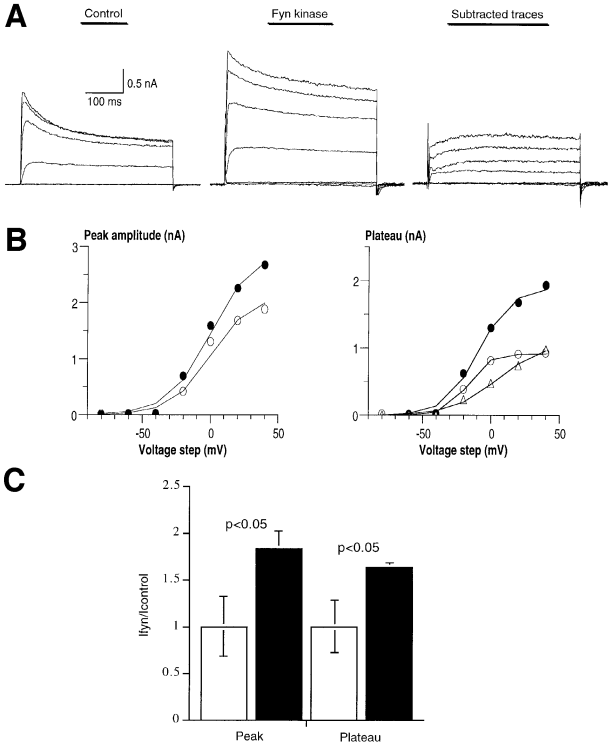

Fig. 4. Upregulation of the K^+ currents by recombinant $p55^{fyn}$ tyrosine kinase. (**A**) Recombinant $p55^{fyn}$ tyrosine kinase (30 U/ml) introduced into the patch pipette together with 5 mM ATP, markedly increased the K^+ currents. Representative recordings from the same cell (out of 5 similar experiments), 1 min (control, left panel) and 6 min (Fyn kinase, middle panel) after establishing the whole-cell configuration are shown. The same activation protocol was used as in Figure 2A. The subtracted traces are shown in the right panel. When either ATP or the Fyn kinase alone was introduced into the patch-recording pipette, no effect was observed on the K^+ currents (not shown). (**B**) The I–V relations of the transient (peak, left) and sustained (plateau, right) components of the currents shown in (A) correspond to recordings obtained 1 min (○) and 6 min (●) after establishing the whole-cell configuration. In the right panel, the I–V relation of the subtracted traces (△) is also shown. (**C**) $I_{fyn}/I_{control}$ corresponds to the ratio of current amplitudes measured at +60 mV and obtained 1 min (open columns) and 6 min (solid columns) after establishing the whole-cell configuration. The $I_{fyn}/I_{control}$ ratios were 1.6 ± 0.05 and 1.8 ± 0.18 for the transient and sustained current components, respectively ($n = 5$).

with two inactivation time constants. At first appearance, herbimycin A caused an acceleration of the whole-cell K^+-current inactivation with τ_1 = 35.0 ± 3.5 ms reduced

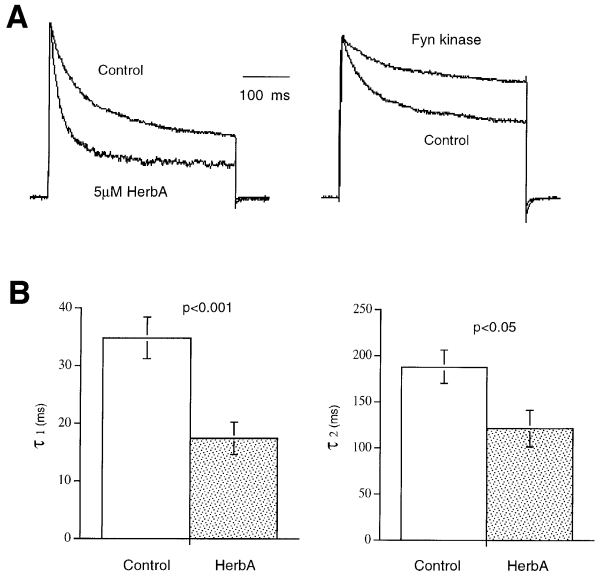

Fig. 5. Herbimycin A and Fyn kinase affect the macroscopic K^+ current kinetics. (**A**) Whole-cell current kinetics recorded from the same cell by stepping membrane potential from –80 to + 60 mV for 400 ms duration before and after 10 min application of 5 μM Herb A (left panel). Recording protocol as in the left panel with 5 mM ATP plus 30 U/ml recombinant $p55^{fyn}$ in the patch pipette, 1 min (control) and 8 min (Fyn kinase) after establishing the whole-cell configuration (right panel). Fyn kinase slowed down the inactivation kinetics. In the example shown τ1 increased from 40 to 71 ms, while τ2 remained the same at ~275 ms. (**B**) The whole-cell inactivation kinetics described by a biexponential function show that 5 μM Herb A significantly reduced the two time constants. τ1 was reduced from 35 ± 3.5 to 17 ± 2.6 ms; τ2 was reduced from 187 ± 18 to 121 ± 18 ms. Data shown are expressed as mean ± SEM (n = 9).

to 17.0 ± 2.9 ms (n = 9) and τ_2 =187 ± 18 ms reduced to 121 ± 20 ms (n = 9) (Figure 5). Conversely, Fyn kinase application caused an apparent slowing down of the current inactivation kinetics with a doubling of the first inactivation time constant τ_1 from ~35 to 70 ms, leaving τ_2 unchanged at >200 ms (Figure 5A, right panel, and data not shown). Taken together, these data suggest that the Fyn kinase action mainly concerns the delayed-rectifier K^+ current, whose increased contribution leads to the observed changes in whole-cell K^+-current kinetics and amplitude.

Kv1.5 and kv2.1 α subunits are constitutively tyrosine phosphorylated in SCs

Demonstration of the constitutive activation of delayed-rectifier K^+ current by Src family tyrosine kinases strongly suggested that certain Kv-channel α subunits may undergo substantial basal tyrosine phosphorylation in SCs. To address this issue, Kv-channel tyrosine phosphorylation was investigated using reciprocal immunoprecipitation–immunoblot analysis with anti-phosphotyrosine and anti-Kv channel antibodies. Among Kv-channel α subunits expressed in SCs, Kv1.5 and Kv2.1 were found to be strongly tyrosine phosphorylated under basal culture conditions (Figures 6A and 7A). Anti-phosphotyrosine antibodies detected very weak and blurred bands when Kv3.1 was immunoprecipitated, while it recognized no bands when precipitation was performed with preimmune serum (Figures 6A and 7A). Consistent with the direct immunoblot analysis (Figure 1A), two main Kv1.5 isoforms of ~65 and 90 kDa were immunoprecipitated from SC membranes by mouse monoclonal or rabbit polyclonal anti-Kv1.5 antibodies (Figure 7A). As suggested in previous work, the 90 kDa isoform could reflect post-translational modifications (Mi *et al*., 1995; Attali *et al*., 1997). Anti-Kv2.1 monoclonal antibodies immunoprecipitated only one major 115 kDa species which was tyrosine phosphorylated (Figure 6A). Reciprocally, both Kv1.5 and Kv2.1 were clearly detected by their respective antibodies among the phosphotyrosine-containing proteins co-precipitated by anti-phosphotyrosine antibodies from SC membranes (Figures 6A and 7A). Pretreatment of SCs with 2.5 μM herbimycin A for 15 min resulted in decrease of >60 and 25% of Kv2.1 and Fyn tyrosine phosphorylation, respectively, as assessed by band densitometry analysis of immunoprecipitations (Figures 6 and 7). In contrast, no significant change in the Kv1.5 tyrosine phosphorylation was found upon herbimycin A treatment (n = 4; Figure 7). As previously described (Bare *et al*., 1993), phosphorylated Fyn appeared as a doublet of 59 and 56 kDa. The lower band could reflect a proteolytic cleavage of $p59^{fyn}$.

Association of Kv channels with Fyn tyrosine kinase in cultured SCs

The opposite effects of herbimycin A and recombinant Fyn kinase on the delayed-rectifier K^+ current raised the possibility of a direct physical interaction between Kv-channel α subunits and Fyn tyrosine kinase. Immunoblot and immunofluorescence analyses showed that Fyn was strongly expressed in SCs (see Figures 1B4, 6B and 7B). When SC membranes were immunoprecipitated with anti-Kv1.5 and anti-Kv2.1 antibodies, a 59 kDa Fyn immunoreactive band was clearly detected on the blots using specific anti-fyn monoclonal antibodies (Figures 6B and 7B). Conversely, Fyn could co-immunoprecipitate with Kv1.5 or Kv2.1 α subunits. Indeed, anti-Kv1.5 and anti-Kv2.1 antibodies specifically detected on blots the respective channel proteins from the immune complexes precipitated by anti-fyn antibodies (Figure 7B and data not shown). In contrast, anti-Kv3.1 antibody recognized specifically a 126 kDa protein in SC membranes, but it did not detect immunoreactive Kv3.1 in Fyn immune complexes (Figure 7B). Figure 6D shows that a tyrosine kinase activity also co-precipitated with Kv2.1 α subunits, as detected by an *in vitro* kinase assay performed on Kv2.1 immune complexes with γ-[^{32}P]ATP and poly (Glu/Tyr, 4:1) used as an exogenous tyrosine kinase substrate. Double immunofluorescence labeling indicated that Fyn was stained as cluster-like patterns that partially overlapped with Kv2.1 immunostaining (Figure 1B). Next, we attempted to elucidate with which domain of Fyn, Kv2.1 could interact. In contrast to Kv1.5, the Kv2.1 subunit does not possess a proline-rich region that could provide a binding site for the SH3 domain of Src family tyrosine kinases (Holmes *et al*., 1996b). In a pull-down assay, we checked whether Kv2.1 could physically bind to the SH2 domain of Fyn. For this purpose, glutathione *S*-transferase (GST)–fyn SH2 domain (145–247) fusion protein coupled to agarose beads was used to bind proteins from SC detergent extracts. Subsequent immunoblotting with anti-Kv2.1 antibodies showed an immunoreactive band of 115 kDa, while agarose beads coupled to GST did not

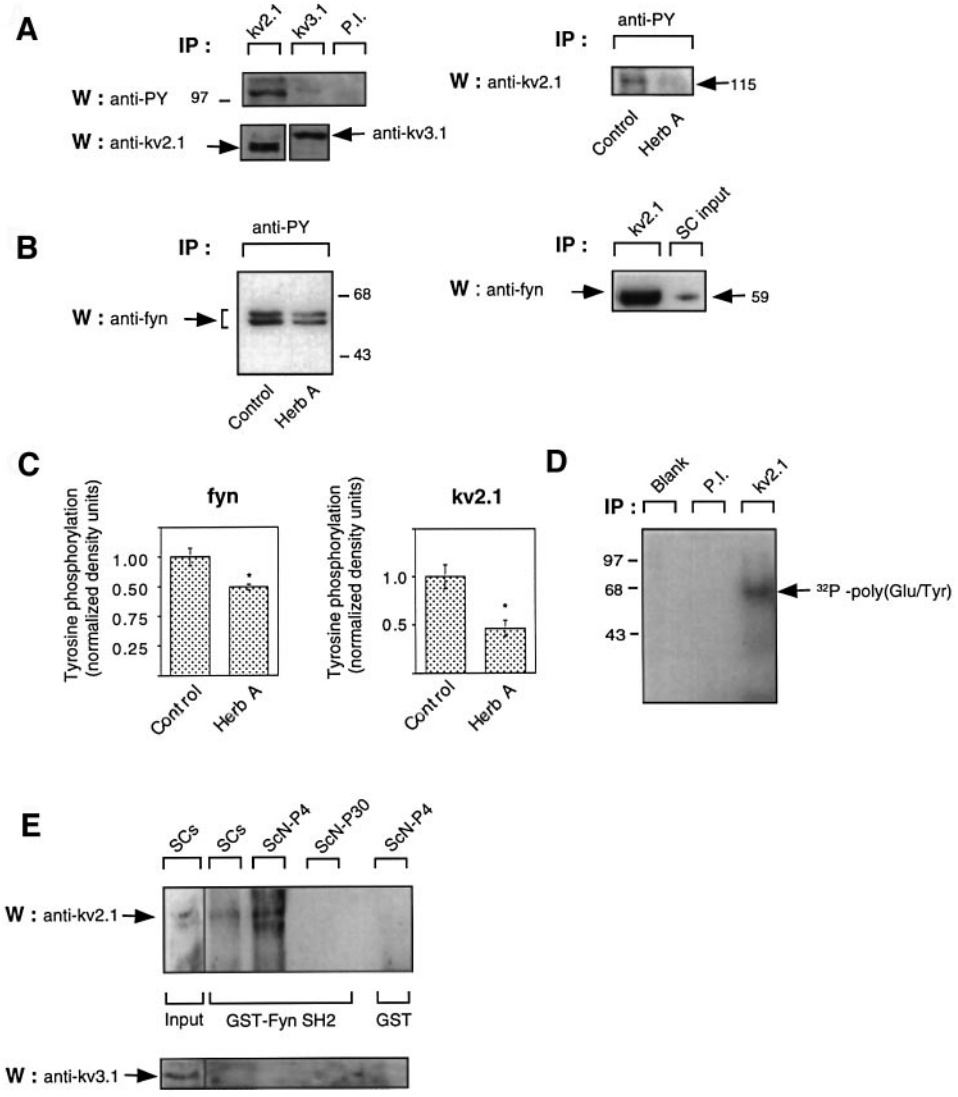

Fig. 6. Tyrosine phosphorylation and association of Kv2.1 with Fyn in Schwann cells. (**A**) Left: SC membranal fractions were subjected to immunoprecipitation with anti-Kv2.1, anti-Kv3.1 or control preimmune (P.I.) antibodies and blots were probed with anti-phosphotyrosine (anti-PY). To verify the presence of channel proteins, blots were stripped and re-probed with the respective anti-Kv antibodies. Right: SCs were treated with 2.5 μM Herb A for 15 min. Reciprocal immunoprecipitation was carried out with anti-PY and blots were probed with either anti-Kv2.1 (A) or anti-fyn (B) antibodies. (**B**) Co-immunoprecipitation of Kv2.1 and Fyn is shown. As a control for Fyn immunoreactivity, a sample of SC membranes (SC input) was run in the same gel. (**C**) Quantitation of the effects of Herb A on tyrosine phosphorylation of Fyn and Kv2.1. Data of densitometric scanning were normalized to values of control cells and represent mean ± SEM of four independent experiments. * Differs significantly from control, $P < 0.01$. (**D**) Tyrosine kinase activity associated with Kv2.1 immune complexes in SCs. Solubilized SC membranes were immunoprecipitated with either anti-Kv2.1 or P.I. antibodies. The immune complexes and sample of solubilization buffer (Blank) were subjected to *in vitro* kinase assays with poly (Glu/Tyr, 4:1) in the presence of 10 μCi [γ-^{32}P]ATP. ^{32}P-incorporated proteins were resolved on 10% SDS–polyacrylamide gel, followed by autoradiography. (**E**) SH2 domain of Fyn mediates its association with Kv2.1. Solubilized SC membranes and homogenates of postnatal (P4) and adult (P30) mice sciatic nerves were incubated with agarose-conjugated GST–Fyn SH2 or GST. Bound proteins were eluted, run on gels and blots were probed with either anti-Kv2.1 or anti-Kv3.1b antibodies.

bind any Kv2.1 immunoreactive protein. No Kv3.1b immunoreactive protein could be pulled-down from SCs extracts by GST–fyn SH2 agarose beads (Figure 6E).

Kv1.5 and Kv2.1 α subunits are tyrosine phosphorylated and associate with Fyn in developing sciatic nerve in vivo

The expression and modulation of Kv channels in SCs could potentially be influenced by the extracellular environment, contact with the axon and the availability of growth factors. Therefore, it was important to evaluate and compare the findings obtained for SCs in culture with those in the sciatic nerve *in vivo*. The same strategy of reciprocal immunoprecipitation–immunoblot analysis was applied to sciatic nerves of 4-day-old postnatal mice (P4), a time reflecting the onset of myelination. As for SCs in culture, Kv1.5, Kv2.1 and Fyn were co-immunoprecipitated by anti-phosphotyrosine antibodies (Figure 8A). Furthermore, in homogenates prepared from P4 mouse sciatic nerves, both Kv1.5 and Kv2.1 were co-immunoprecipitated by the antibody to Fyn, but not by pre-immune antibodies (Figure 8B). Interestingly, tyrosine phosphorylation of Fyn in sciatic nerve was maximal during initial stage of myelination (P4) and declined thereafter (P30) by >50%, although the steady-state level of Fyn protein expression did not change (Figure 8A). Pull-down experiments

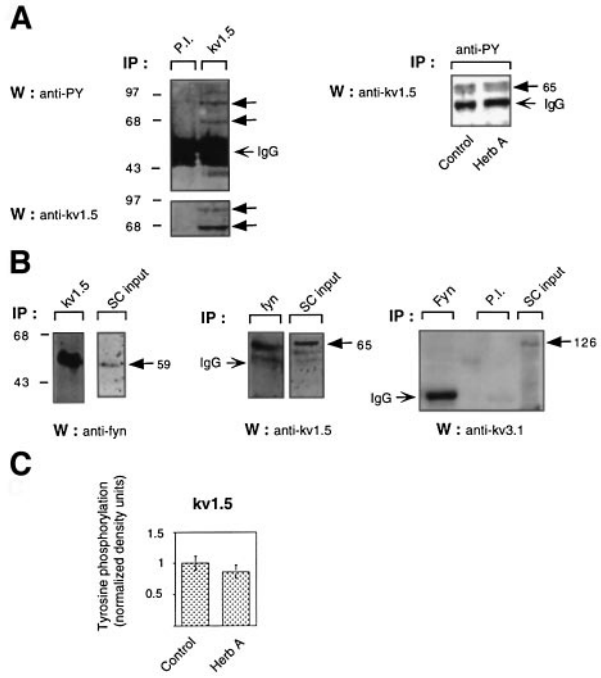

Fig. 7. Tyrosine phosphorylation and association of Kv1.5 with Fyn in Schwann cells. (**A**) Tyrosine phosphorylation of Kv1.5 in SCs. Herb A treatment, reciprocal immunoprecipitations with anti-Kv1.5, anti-phosphotyrosine (anti-PY) or P.I antibodies; immunoblotting and re-probing were performed as described for Kv2.1 in Figure 6. Non-specific bands corresponding to immunoglobulin heavy chain (IgG) are also observed. (**B**) Reciprocal co-immunoprecipitations of Kv1.5 and Fyn in SCs. No Kv3.1b immunoreactive protein could be detected in fyn immune complexes. Membranal inputs (~10%) were used, as positive control. (**C**) Quantitation of tyrosine phosphorylation of Kv1.5 in control and Herb A-treated SCs, as described in Figure 6.

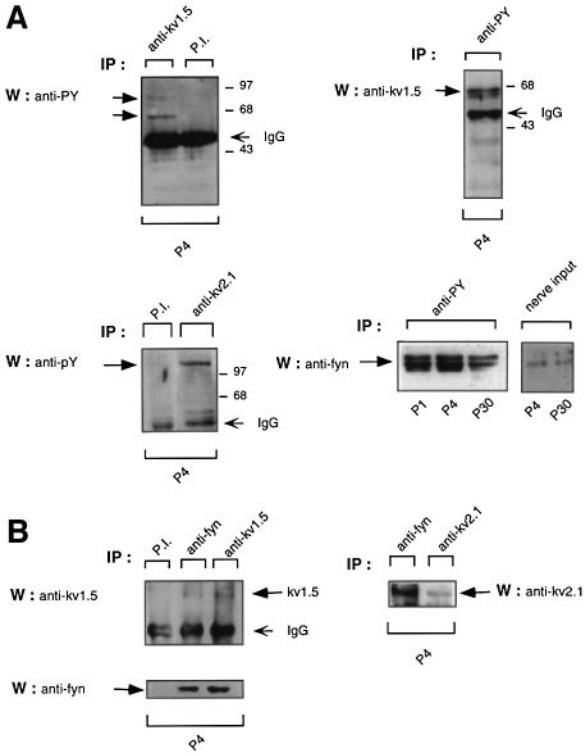

Fig. 8. Tyrosine phosphorylation and interaction of Kv1.5 and Kv2.1 with Fyn in sciatic nerve. (**A**) Tyrosine phosphorylation of Kv1.5, Kv2.1 and Fyn. Homogenates of acutely isolated sciatic nerves from P4 mice were subjected to immunoprecipitation with anti-Kv1.5, anti-Kv2.1 or preimmune (P.I.) antibodies and blots were probed with anti-phosphotyrosine (anti-PY). Tyrosine phosphorylation of Kv1.5 in P4 sciatic nerve is also demonstrated by reciprocal immunoprecipitation with anti-PY and immunoblot with anti-Kv1.5. Tyrosine phosphorylation of Fyn, detected in P1, P4 and P30 sciatic nerves is also shown along with Fyn protein inputs. (**B**) Reciprocal co-immunoprecipitation of Fyn with Kv1.5 and Kv2.1 in P4 sciatic nerve is shown. Following the probing with anti-channel antibodies (to Kv1.5 and Kv2.1), blots were stripped and re-probed with anti-fyn.

showed that the SH2 domain of Fyn bound specifically to Kv2.1 subunits in P4 old-sciatic nerve extracts, as revealed by the Kv2.1 immunoreactive doublet of 105 and 115 kDa (Figure 6E). In contrast, very few if any Kv2.1 immunoreactive protein could be pulled-down in P30-old sciatic nerve extracts by GST–fyn SH2 agarose beads (Figure 6E).

Blocking tyrosine kinases and voltage-gated K^+ channels inhibits SC proliferation

Voltage-gated K^+ channels were suggested to be linked to mitogenesis in various glial cells including SCs, astrocytes and oligodendrocyte progenitors (Chiu and Wilson, 1989; Konishi, 1989; Pappas *et al*., 1994; Attali *et al*., 1997). Similarly, tyrosine kinases were recognized to play a role in the development and proliferation of glial cells (Trotter *et al*., 1989; LeBeau *et al*., 1991; Bare *et al*., 1993). Thus, we examined whether inhibition of tyrosine kinases or blockade of K^+ channels affects SC proliferation as measured by [^{3}H]thymidine incorporation. Purified SCs cultured in the presence of 10% fetal calf serum (FCS) were assayed for proliferation one day after plating by addition of [^{3}H]thymidine (0.2 μCi/well) for a 24 h incorporation period in the presence or absence of blockers. Serum deprivation (0.3% FCS) inhibited SC proliferation by 72 ± 2% (n = 3; Figure 9). In the presence of 1 mM 4-AP, a concentration found to block >80% of the transient component of voltage-gated K^+ currents in mouse SC (Konishi, 1989; data not shown), there was a 35 ± 11% (n = 3) inhibition of SC proliferation. When 50 μM quinidine was added to the incubation medium, 93 ± 1% of SC proliferation was blocked (n = 3); at this concentration, quinidine inhibited by >80% both the transient and sustained components of SC K^+ currents (Figures 2A and 9). Herbimycin A treatment caused a dramatic dose-dependent inhibition of SC proliferation, reaching ~50% at 5 nM and a complete block of proliferation was obtained in the micromolar range. It is worth noting that all blockers used did not produce toxic effects at the above working concentrations.

Discussion

Our work provides the first evidence of a functional linkage between Src family tyrosine kinases and activation of voltage-gated K^+ channels in glial cells. Regarding the limited data available so far on native Kv-channel subunit modulation, this study adds novel insights into the regulation of K^+ channels by Src tyrosine kinases. Our data indicate that a Src family tyrosine kinase constitutively activates delayed-rectifier K^+ channels (I_K) in mouse SCs. Among the kinase substrate candidates, the Kv-channel α subunits Kv1.5 and Kv2.1 are found to be constitutively tyrosine phosphorylated and to physically associate with

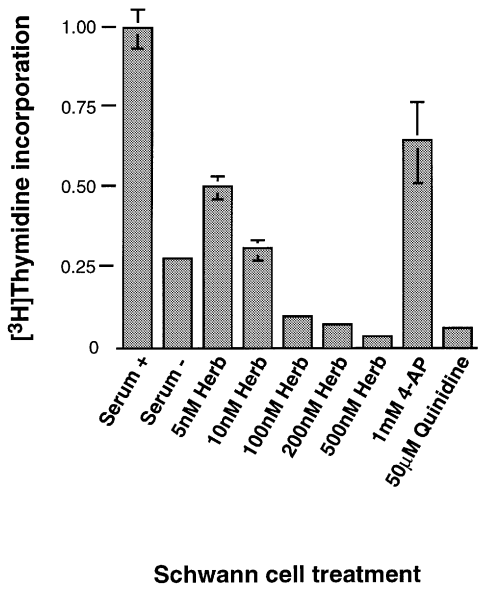

Fig. 9. Effect of herbimycin A and Kv-channel blockers on Schwann cell proliferation. [^{3}H]Thymidine incorporation (0.2 μCi/well) was assayed in cultured SCs exposed for 24 h to either 1 mM 4-AP, 50 μM quinidine or various concentrations of Herb A (5 nM–0.5 μM) in the presence of 10% FCS. Effect of serum deprivation (0.3% for 24 h) on SC proliferation is also shown. The results were normalized to the maximal serum-stimulated proliferation. Data points represent the mean ± SEM of three independent experiments, each performed in triplicate.

Fyn both in cultured SCs and in the sciatic nerve *in vivo*. In addition, inhibition of SC proliferation by a tyrosine kinase inhibitor and by K^+-channel blockers suggests that the modulation of I_K channels by Src tyrosine kinases could be important for SC proliferation and the onset of myelination.

A Src family tyrosine kinase constitutively activates delayed-rectifier K^+ currents: effects of herbimycin A, genistein and recombinant p55^{fyn}

Most of the recent studies accumulated so far on K^+-channel modulation by tyrosine kinases refer to heterologous expression either in *Xenopus* oocytes or in transfected cells and indicate that tyrosine kinase activation leads to an inhibition of the K^+ currents. Stimulation of the muscarinic m1 AChR by carbachol is shown to reduce potently the amplitude of Kv1.2 currents in HEK 293 cells and *Xenopus* oocytes (Huang *et al*., 1993). More recently, a novel non-receptor tyrosine kinase called PYK2 is found to directly phosphorylate Kv1.2 leading to a rapid suppression of the K^+ current in *Xenopus* oocytes (Lev *et al*., 1995). Transactivation of EGF receptor is shown to link m1 AChR to Kv1.2 suppression (Tsai *et al*., 1997). Similarly, when Kv1.3 or Kv1.5 is expressed in HEK 293 cells with v-Src or epidermal growth factor (EGF) receptors (stimulated by EGF), the current amplitude is depressed due to robust phosphorylation of the respective channel proteins (Holmes *et al*., 1996a,b; Bowlby *et al*., 1997).

In contrast, we find that voltage-dependent K^+ currents in SCs are constitutively activated by a Src family tyrosine kinase since they are suppressed by the tyrosine kinase inhibitors herbimycin A and genistein and they are potently upregulated when recombinant Fyn kinase (p55^{fyn}) is internally applied to SCs. Our findings contrast with many other reports showing an inhibition of Kv-channel activity by tyrosine kinases (Huang *et al*., 1993; Lev *et al*., 1995; Holmes *et al*., 1996a,b; Szabo *et al*., 1996; Bowlby *et al*., 1997; Tsai *et al*., 1997). This apparent discrepancy may reflect marked differences in cellular background (e.g. absence of regulatory channel subunits in heterologous host cells versus native cells). In addition, all previous studies have been conducted on cells heterologously expressing Kv1-channel subclasses, mainly Kv1.2, Kv1.3 and Kv1.5. It is possible that the differences in channel modulation found in SCs are accounted for by the tyrosine phosphorylation of the Kv2.1-channel subclass (see below). To our knowledge, this is the first study describing the regulation of Kv2.1 channel by tyrosine kinases. Interestingly, our data are in line with a recent work carried out on native channels showing that insulin enhances a delayed-rectifier K^+ current in *Aplysia* bag-cell neurons (Jonas *et al*., 1996). Likewise, tyrosine kinase stimulation via prolactin receptor signaling was shown to activate a voltage-dependent Ca^{2+}-sensitive K^+ channel (Prevarskaya *et al*., 1995).

In SCs, the delayed-rectifier component I_K appears to be the main target of Src family tyrosine kinase activation. At first appearance, herbimycin A and recombinant p55^{fyn} treatments lead to an acceleration and a slowing down of the whole-cell inactivation kinetics, respectively. However, analyses of the subtracted traces point to I_K as the main component affected by the Src family tyrosine kinase, leaving a smaller contribution, if any, to I_A. The voltage-dependence of activation and inactivation is unaffected but it remains possible that Src family tyrosine kinases control the number of available active channels. Alternatively, the tyrosine phosphorylation process could increase the channel open probability, P_o, as previously described for NMDA receptors (X.-M.,Yu *et al*., 1997). Basal modulation of K^+ channels by phosphorylation implies that there are constitutively active kinases interacting directly or indirectly with Kv-channel subunits. What could activate Src family tyrosine kinases in SCs? Growth factor receptor tyrosine kinases are known to activate Src family members (Erpel and Courtneidge, 1995). Platelet-derived growth factor (PDGF) or Insulin-like growth factor 1 (IGF1) receptors which are expressed in SCs are potential candidates (Mirsky and Jessen, 1996; Stewart *et al*., 1996; Zorick and Lemke, 1996). Src family tyrosine kinases could be activated by some other upstream kinase, such as protein kinase C (PKC), however we were unable to detect such a modulation using phorbol esters as PKC activators (unpublished results). Noteworthy, association with the substrate itself may keep the kinase in its activated state (Moarefi *et al*., 1997). Regarding the identity of the Src family kinase involved in I_K activation, Fyn is a plausible though not exclusive candidate. Indeed, the Kv-channel α subunits Kv1.5 and Kv2.1 clearly associate with Fyn in cultured SCs and in the sciatic nerve. However, other classes of tyrosine kinases may be also involved. Finally, we cannot exclude activation of a downstream tyrosine kinase whose final substrate would be the Kv-channel subunits. For example, a recent study showed that PYK2 is activated by Fyn during T cell antigen receptor signaling (Qian *et al*., 1997).

The Kv-channel α subunits as substrate candidates for Fyn tyrosine kinase in SCs

We and others are able to identify at the mRNA and protein levels the Kv1.1, Kv1.2, Kv1.4, Kv1.5, Kv2.1 and Kv3.1b-channel α subunits in rat and mouse SCs and sciatic nerve (Figure 2; Chiu *et al*., 1994; Mi *et al*., 1995; Sobko,A., Peretz,A., Shirihai,O., Etkin,S., Cherepanova,V., Dagan,D. and Attali,B., in preparation). Our findings suggest that Kv1.5 and Kv2.1 α subunits are likely to be substrate candidates of the Fyn tyrosine kinase for the following reasons: (i) Kv1.5 and Kv2.1 are subject to robust constitutive tyrosine phosphorylation in cultured SCs, while Kv1.2, Kv1.4 and Kv3.1b subunits are not (Figures 6 and 7; data not shown). (ii) Kv1.5 and Kv2.1 physically associate with Fyn in SCs, while Kv3.1b do not. Along the same lines, X.-M.,Yu *et al*. (1997) also show that Kv3.1 does not co-precipitate with Src in the brain. (iii) Kv1.5 and Kv2.1 are also constitutively tyrosine phosphorylated and co-precipitate with Fyn in the P4 sciatic nerve *in vivo*. Considering the Kv1.5 subunit as a possible substrate, it has the molecular attributes for being tyrosine phosphorylated, notably at its N-terminus. In addition, the mouse and human versions of Kv1.5 possess within their N-terminal region, a proline-rich domain which could provide a binding site for the SH3 motif of Src family tyrosine kinases (Holmes, 1996b). However, it should be noted that herbimycin A treatment does not significantly reduce the level of Kv1.5 phosphotyrosine (Figure 7). Furthermore, in view of previous work performed in transfected HEK 293 cells (Holmes, 1996b) one would expect a suppression rather than an activation of the K^+ currents by the Src tyrosine kinase. This suggests that either Kv1.5 is not the target of the Src family kinase-mediated activation of I_K in SCs or alternatively, the nature of the modulation is very different in native Kv1.5 channels. Considering the Kv2.1 subunit, it is interesting to note that it contains within its N-terminal region a consensus site for Src family-mediated tyrosine phosphorylation at position 121–126 (DEIYLE, consensus XEIYXE). Upon phosphorylation, it could provide an interacting site for Src family tyrosine kinase via SH2 domain (Songyang *et al*., 1993, 1995; Cantley and Songyang, 1997). Indeed, Kv2.1 interacts with the SH2 domain of Fyn, as illustrated by the pull-down experiments. Kv2.1 exhibits a robust tyrosine phosphorylation which is inhibited by herbimycin A treatment. Furthermore, Kv2.1 interacts with Fyn kinase in cultured SCs as well as in the P4 sciatic nerve and a tyrosine kinase activity co-precipitates with Kv2.1 α subunits, as detected by an *in vitro* kinase assay performed on Kv2.1 immune complexes (Figure 6). Taken together, these data strongly suggest that Kv2.1 subunits are best suited for being modulated by Src family tyrosine kinases in SCs. In heterologous expression, the threshold for activation of homomultimeric Kv2.1 channels is within the –20 mV range (Frech *et al*., 1989), a value more depolarized to that of the native I_K in SCs (–50 mV). Interestingly, recent studies suggest that native Kv2 channels may be built-up of heteromultimeric complexes, comprising β subunits and electrically silent α subunits (Fink *et al*., 1996; Hugnot *et al*., 1996; Patel *et al*., 1997; Salinas *et al*., 1997a,b). A recent member of this new family, Kv9.3, has been cloned and is found to be homologous to Kv2.1 subunit (Patel *et al*., 1997). Although encoding an electrically silent K^+ channel, Kv9.3 upon co-expression with Kv2.1 increases K^+-current amplitude and shifts the threshold of activation from –20 mV to –50 mV (Patel *et al*., 1997). In this regard, it is tempting to speculate that the native I_K in SCs could partly correspond to an heteromultimeric channel complex of Kv2.1 and Kv9.3 subunits activating above –50 mV and being robustly modulated by Src family tyrosine kinases. Future work should test this assumption.

Functional significance of Src family kinase-mediated activation of I_K in Schwann cell development

Non-receptor tyrosine kinases of the Src family such as Src and Fyn, are shown to play important role in the initiation of mitosis and in apoptosis, the latter being considered as 'abortive mitosis' (Erpel and Courtneidge, 1995; Migita *et al*., 1995; Roche *et al*., 1995; Atkinson *et al*., 1996). Premyelinating SCs are characterized by an increased expression of voltage-dependent K^+ currents (Wilson and Chiu, 1990) and high levels of activated Fyn kinase (Bare *et al*., 1993; Umemori *et al*., 1994). Fyn activation is shown to be an important feature of early myelination and Fyn-deficient mice exhibit impaired myelination (Umemori *et al*., 1994). Several lines of evidence suggest the existence of overlapping signals in the regulation of proliferation and myelin differentiation (Mirsky and Jessen, 1996). Our study raises the possibility that Fyn activation could coincide with outward K^+ current upregulation during SC development. In postnatal nerves prior to myelination and during nerve regeneration, this increase in outward K^+ current may mediate SC proliferation. Indeed, Kv-channel blockers are well-known inhibitors of SC proliferation (Chiu and Wilson, 1989; Pappas and Ritchie, 1998). In this work, we show that herbimycin A inhibits outward K^+ currents, decreases tyrosine phosphorylation of the Kv2.1-channel subunit and Fyn kinase itself and potently blocks the proliferation of SCs. Naturally, our data do not imply that the herbimycin A antiproliferative activity arises exclusively from its inhibition of I_K currents. However, a functional linkage could exist between Kv channels and the Src family kinase activities, which might be required to keep SC proliferative ability. In agreement with this prediction, glial cells expressing constitutively active v-Src were reported to display strong outward K^+ currents (Trotter *et al*., 1989). On the other hand, a prolonged Fyn-mediated Kv-channel activation may lead to an excessive loss of potassium, and ultimately to apoptosis. In this regard, increase of the delayed-rectifier K^+ current results in apoptosis of mouse neocortical neurons (S.P.,Yu *et al*., 1997). Importantly, SC precursors and premyelinating SCs have been shown to undergo programmed cell death *in vitro*. This might also be the case *in vivo* in order to reach a 1:1 ratio with associated axonal internodes (Jessen *et al*., 1994; Grinspan *et al*., 1996; Syroid *et al*., 1996; Trachtenberg and Thompson, 1996). Along this line, it is interesting to note that the tyrosine phosphorylation of Kv2.1 is apparently much weaker in P30 than in P4 sciatic nerves, as revealed by the pull-down experiments. According to this scenario, subsequent developmental decrease in Fyn kinase activity and outward K^+ currents could contribute to the exit of SCs from the cell cycle and the onset of myelination.

Materials and methods

Materials

The recombinant Fyn kinase ($p55^{fyn}$) was purchased from Upstate Biotechnology (Lake Placid, NY). Herbimycin A (Herb A), poly (Glu/Tyr, 4:1), quinidine, protein A/G–Sepharose were from Sigma. The source of antibodies was as follows: monoclonal and polyclonal antibodies to Kv1.2, Kv1.4, Kv1.5, Kv2.1 and anti-phosphotyrosine 4G10 were from Upstate Biotechnology. Anti-Kv1.5 and anti-Kv3.1b polyclonal antibodies were purchased from Alomone Labs (Jerusalem, Israel). Monoclonal antibody to Fyn (sc-434) and GST–fyn SH2 fusion protein-coupled agarose beads (sc-4042) were obtained from Santa Cruz Biotechnology (Santa Cruz, CA). Rabbit anti-S-100 was from Sigma. Goat anti-mouse, goat anti-rabbit fluorescein (FITC)- or rhodamine (TRITC)-conjugated and horseradish peroxidase-conjugated secondary antibodies were from Jackson Laboratories (West Grove, PA). γ-[^{32}P]ATP (3000 Ci/mmol) was purchased from Amersham.

Schwann cell cultures, proliferation and immunocytochemistry

Primary SC cultures were prepared from P4 postnatal mouse sciatic nerves according to Brockes *et al*. (1979). Cells were plated on poly-D-lysine-coated Petri dishes or glass coverslips and grown in Dulbecco's modified Eagles medium (DMEM)/F12 supplemented with 2 mM glutamine, 10% FCS and antibiotics. Under these conditions, which allowed proliferation and inhibited the expression of the myelin phenotype, we obtain 90–95% of pure Schwann cell cultures, as controlled by S-100 immunofluorescence. For [^{3}H]thymidine incorporation, cells were treated with various concentrations of channel blockers or Herb A, as indicated and the assay was carried out, as previously described (Attali *et al*., 1997). When cells were treated with Herb A, carrier alone (0.1% DMSO) was used as control. Immunocytochemistry was carried out (Attali *et al*., 1997) and cells were viewed using a Zeiss Axioplan microscope equipped with phase contrast and epifluorescent optics.

Preparation of cell lysates and membrane solubilization

Confluent cell cultures (60 or 100 mm dishes) were washed twice with cold phosphate-buffered saline (PBS) and scraped on ice in PBS, containing 1 mM phenylmethyl sulphonylfluoride (PMSF). When samples were used for phosphorylation studies, 50 mM sodium fluoride and 5 mM sodium orthovanadate were added to the buffers in order to block endogenous phosphatases. Following centrifugation, cell pellets or acutely isolated sciatic nerves were either frozen in liquid nitrogen and kept at –80°C until use, or homogenized in the buffer containing 50 mM Tris pH 7.4, 1 mM ethylenediaminetetraacetic acid (EDTA), 1 mM PMSF, 10 μg/ml aprotinin and 10 μg/ml leupeptin and centrifuged at 21 000 *g* for 30 min at 4°C. The pellet (crude membranal fraction) was sonicated and resuspended either in SDS–sample buffer (Laemmli, 1970) for direct immunoblot analysis or in the solubilization buffer (glycerol 10 %, 50 mM HEPES pH 7.4, 10 mM EDTA, NaCl 150 mM, 1.5 mM $MgCl_2$, 1% Triton X-100, 1 mM PMSF, 10 μg/ml aprotinin, 10 μg/ml leupeptin) for immunoprecipitation. Protein concentration was determined using Bio-Rad protein assay solution with bovine serum albumin and human immunoglobulin as a standard.

Immunoprecipitation

Samples were incubated under shaking in the solubilization buffer for 1 h at 4°C and spun at 21 000 *g*. The extract (supernatant) was precleared with 1:1 slurry of protein A/G–Sepharose (30 μl per ml of extract) equilibrated in lysis buffer, for 1 h at 4^0C under shaking. After a short spin, the supernatant was transferred into a new tube and incubated under shaking with the antibodies or the respective preimmune serum at 4°C for 4 h or overnight. Immune complexes were pooled-down after the addition of 30 μl of protein A/G–Sepharose for 1 h at 4°C under shaking. Immunoprecipitates were washed three times in the solubilization buffer and beads were finally resuspended in 30 μl 2× SDS–sample buffer, boiled at 100°C for 5 min to elute the precipitated proteins. The eluent was electrophoresed on SDS–10% polyacrylamide gel along with standard mol. wt markers.

Immunoblot analysis

After separation on SDS–polyacrylamide gels, proteins were electrotransferred to nitrocellulose blots. Blots were blocked in PBS containing 10% non-fat milk and 0.05% Tween 20 (Western buffer) for 1 h at room temperature under shaking. Then blots were incubated with the respective antibody overnight at 4°C or for 4 h at room temperature. After three washes with Western buffer, blots were incubated for 1 h with horseradish peroxidase (HRP)-conjugated secondary antibody, followed by extensive washes in PBS. Labeled proteins were detected by enhanced chemiluminescence (ECL, Amersham). Band signals corresponding to immunoreactive proteins were measured and scanned by image densitometry, using NIH Image 1.54 and Adobe Photoshop 3.0 software.

Kinase assays

Immune complexes precipitated by anti-Kv2.1 antibodies and protein A/G–Sepharose were washed twice with immunoprecipitation buffer and once with kinase buffer [20 mM HEPES pH 7.4, 50 mM NaCl, 10 mM $MgCl_2$, 5 mM $MnCl_2$, 20 mM Tris–HCl pH 7.4, 0.1 mM dithiothreitol (DTT) and protease/phosphatase inhibitor mix], and incubated with 30 μl kinase buffer containing 25 μg poly(Glu/Tyr) (4:1) and 10 μCi γ-[^{32}P]ATP for 15 min at 37°C. The reaction was stopped by adding 15 μl SDS sample buffer and by boiling the sample for 5 min.

GST–Fyn SH2 fusion pull-down experiments

The mouse Fyn SH2 domain (amino acids 145–247)–GST fusion protein and control GST protein conjugated to agarose beads were used for pull-down experiments. Membranes solubilized in the lysis buffer were mixed with 10 μg of agarose-conjugated GST fusion protein and incubated for 3 h at 4°C under shaking. Beads were washed once with solubilization buffer, and three times with PBS containing 1% Triton. The bound proteins were eluted by adding SDS sample buffer and subjected to Western blot analysis with antibodies to Kv channels.

Electrophysiology

Cultured SCs, plated on poly-D-lysine-coated glass coverslips were placed in a 1 ml recording chamber mounted on the stage of a Zeiss Axiovert 35 inverted microscope. The whole-cell configuration of the patch–clamp technique (Hamill *et al*., 1981) was used to record the macroscopic whole-cell currents at room temperature (22 ± 1°C). Signals were amplified using an Axopatch 200B patch–clamp amplifier (Axon Instruments), filtered below 1 KHz via a 4-pole Bessel low pass filter. Data were sampled at 4 KHz and analyzed using pClamp 6.0.2 software (Axon Instruments) and IBM-compatible 486 computer in conjunction with a DigiData 1200 interface (Axon Instruments). The patch pipettes were pulled from borosilicate glass (fiber filled) with resistance of 5–10 MΩ and were filled with (in mM): 120 KCl, 2 $MgCl_2$, 1 $CaCl_2$, 11 EGTA, 10 HEPES, 11 glucose with pH 7.4. For experiments with recombinant Fyn kinase, 5 mM ATP were included to the intracellular recording solution. The external solution contained (in mM): 140 NaCl, 5 KCl, 5 $CaCl_2$, 2 $MgCl_2$, 11 glucose, 10 HEPES with pH 7.4. Series resistances were within 10–16 MΩ and and were compensated by 85–90%. Traces were leak subtracted by the Clampfit program of the pClamp 6.02 software and further analyzed by the Axograph 3.0 software (Axon Instruments). Activation and steady-state inactivation curves were fitted by the Boltzmann distribution (assuming reversal potential of –85mV, calculated by Nernst equation):

$$I/I_{max} = a/\{1+\exp[(V_{50}-V_K)/s]\}$$

where V_{50} is the half maximal activation (for the steady-state activation protocol), or the voltage at which half of the steady-state inactivation was removed and s is the slope of the curve. The transient and the sustained components of the K^+ currents were measured at the peak and the end (400 ms) of the depolarizing traces, respectively. All data were expressed as mean ± SEM. Statistically significant differences were assessed by Student's *t*-test.

Acknowledgements

We would like to thank Drs Vivian Teichberg, Elior Peles and Sima Lev for critical reading of the manuscript and helpful discussions. This research was supported by grants from the Israel Academy of Science, the Minerva Foundation and EEC Bio4-97–2207 (to B.A). A.P. was supported by a Weizmann Institute post-doctoral. B.A is an incumbent of the Philip Harris and Gerald Ronson Career Development chair.

References

Amedee,T., Ellie,E., Dupouy,B. and Vincent,J.D. (1991) Voltage-dependent calcium and potassium channels in Schwann cells cultured from dorsal root ganglia of the mouse. *J. Physiol.*, **441**, 35–56.

Atkinson,E.A., Ostergaard,H., Kane,K., Pinkosi,M., Caputo,A. and Olszowy,M.J. (1996) A physical interaction between the cell death protein Fas and the tyrosine kinase p59fynT. *J. Biol. Chem.*, **271**, 5968–5971.

Attali,B., Wang,N., Kolot,A., Sobko,A., Cherepanov,V. and Soliven,B. (1997) Characterization of delayed rectifier Kv channels in oligodendrocytes and progenitor cells. *J. Neurosci.*, **17**, 8234–8245.

Bare,D.J., Lauder,J.M., Wilkie,M.B. and Maness,P.F. (1993) p59fyn in rat brain is localized in developing axonal tracts and subpopulations of adult neurons and glia. *Oncogene*, **8**, 1429–1436.

Barres,B.A., Chun,L.L.Y. and Corey,D.P. (1990) Ion channels in vertebrate glia. *Annu. Rev. Neurosci.*, **13**, 441–474.

Bekele-Arcuri,Z., Matos,M.F., Manganas,L., Strassle,B.W., Monaghan, M.M., Rhodes,K.J. and Trimmer,J.S. (1996) Generation and characterization of subunit-specific monoclonal antibodies to K+ channel α- and β-subunit polypeptides. *Neuropharmacology*, **35**, 851–865.

Bolen,J.P. (1993) Nonreceptor tyrosine protein kinases. *Oncogene*, **8**, 2025–2031.

Bowlby,M.R., Fadool,D.A., Holmes,T.C. and Levitan,I.B. (1997) Modulation of the Kv1.3 potassium channel by receptor tyrosine kinases. *J. Gen. Physiol*, **110**, 601–610.

Boxall,A.R. and Lancaster,B. (1998) Tyrosine kinases and synaptic transmission. *Eur. J. Neurosci.*, **10**, 2–7.

Brockes,J.P., Fields,K.L. and Raff,M.C. (1979) Studies on cultured rat Schwann cells. I. Establishment of purified populations from cultures of peripheral nerve. *Brain Res.*, **165**, 105–118.

Cantley,L.C. and Songyang,Z. (1997) Specificity in protein–tyrosine kinase signaling. In Corbin,J. and Francis,S. (eds), *Signal Transduction in Health and Disease. Advances in Second Messenger and Phosphoprotein Research*. Lippincott-Raven Publishers, PA, pp. 41–48.

Chiu,S.Y. (1991) Functions and distribution of voltage-gated sodium and potassium channels in mammalian Schwann cells. *Glia*, **4**, 541–558.

Chiu,S.Y. and Wilson,G.F. (1989) The role of potassium channels in Schwann cell proliferation in Wallerian degeneration of explant rabbit sciatic nerve. *J. Physiol.*, **408**, 199–222.

Chiu,S.Y., Scherer,S.S., Blonski,M., Kang,S.S. and Messing,A. (1994) Axons regulate the expression of Shaker-like potassium channel genes in Schwann cells in perpheral nerve. *Glia*, **12**, 1–11.

Courtneidge,S.A. and Fumagalli S. (1994) A mitotic function for Src? *Trends Cell Biol.*, **4**, 337–345.

Du,J., Zhang,L. Weiser,M., Rudy,B. and McBain,C.J. (1996) Developmental expression and functional characterization of the potassium-channel subunit kv3.1b in parvalbumin-containing interneurons of the rat hippocampus. *J. Neurosci.*, **16**, 506–518.

Erpel,T. and Courtneidge,S.A. (1995) Src family protein tyrosine kinases and cellular signal tranduction pathways. *Curr. Opin. Cell Biol.*, **7**, 176–182.

Fadool,D.A., Holmes,T.C., Berman,K., Dagan,D. and Levitan,I.B. (1997) Tyrosine phosphorylation modulates current amplitude and kinetics of a neuronal voltage-gated potassium channel. *J. Neurophysiol.*,**78**, 1563–1573.

Fink,M., Duprat,F., Lesage,F., Heurteaux,C., Romey,G., Barhanin,J. and Lazdunski,M. (1996) A new K^+ channel β subunit to specifically enhance Kv2.2 (CDRK) expression. *J. Biol. Chem.*, **271**, 26341–26348.

Frech,G.C., VanDongen,A.M., Schuster,G., Brown,A.M. and Joho,R.H. (1989) A novel potassium channel with delayed rectifier properties isolated from rat brain by expression cloning. *Nature*, **340**, 642–645.

Fuhrer,C., Sugiyama,J.E., Taylor,R.G. and Hall,Z.W. (1997) Association of muscle-specific kinase MuSK with the acetylcholine receptor in mammalian muscle. *EMBO J.*, **16**, 4951–4960.

Grant,S.G., O'Dell,T.J., Karl,K.A., Stein,P.L., Soriano,P. and Kandel,E.R. (1992) Impaired long-term potentiation, spatial learning and hippocampal development in Fyn mutant mice. *Science*, **258**, 1903–1910.

Grinspan,J.B., Marchionni,M.A., Reeves,M., Coulaloglou,M. and Scherer,S.S. (1996) Axonal interactions regulate Schwann cell apoptosis in developing peripheral nerve: neuregulin receptors and the role of neuregulins. *J. Neurosci.*, **16**, 6107–6118.

Hamill,O.P., Marty,A., Neher,E., Sakmann,B. and Sigworth,F.J. (1981) Improved patch–clamp techniques for high-resolution current recording from cells and cell-free membrane patches. *Pflug. Arch.*, **391**, 85–100.

Holmes,T.C., Fadool,D.A. and Levitan,I.B. (1996a) Tyrosine phosphorylation of the Kv1.3 potassium channel. *J. Neurosci.*, **16**, 1581–1590.

Holmes,T.C., Fadool,D.A., Ren,R. and Levitan,I.B. (1996b) Association of Src tyrosine kinase with a human potassium channel mediated by SH3 domain. *Science*, **274**, 2089–2091.

Hoppe,D., Lux,H.-D., Schachner,M. and Kettenmann,H. (1989) Activation of K^+ currents in cultured Schwann cells is controlled by extracelllar pH. *Eur. J. Physiol.*, **415**, 22–28.

Huang,X.-Y., Morielli,A.D. and Peralta,E.G. (1993) Tyrosine kinase-dependent suppression of a potassium channel by the G protein-coupled m1 muscarinic acetylcholine receptor. *Cell*, **75**, 1145–1156.

Hugnot,J.P., Salinas,M., Lesage,F., Guillemare,E., de Weille,J., Heurteaux,C., Mattei,M.G. and Lazdunski,M. (1996) Kv8.1, a new neuronal potassium channel subunit with specific inhibitory properties towards *Shab* and *Shaw* channels. *EMBO J.*, **15**, 3322–3331.

Jessen,K.R., Brennan,A., Morgan,L., Mirsky,R., Kent,A., Hashimoto,Y. and Gavrilovic,J. (1994) The Schwann cell precursor and its fate: a study of cell death and differentiation during gliogenesis in rat embryonic nerves. *Neuron*, **12**, 509–527.

Jonas,E.A. and Kaczmarek,L.K. (1996) Regulation of potassium channels by protein kinases. *Curr. Opin. Neurobiol.*, **6**, 318–323.

Jonas,E.A., Knox,R.J., Kaczmarek,L.K. and Schwartz,J.H. (1996) Insulin receptor in Aplysia neurons: characterization, molecular cloning and modulation of ion currents. *J. Neurosci.*, **16**, 1645–1658.

Kohr,G. and Seeburg,P.H. (1996) Subtype-specific regulation of recombinant NMDA receptor-channels by protein tyrosine kinases of the Src family. *J. Physiol.*, **492.2**, 445–452.

Konishi,T. (1989) Voltage-dependent potassium channels in mouse Schwann cells. *J.Physiol.*, **411**, 115–130.

Laemmli,E.K. (1970) Cleavage of structural proteins during the assembly of the head of bacteriophage T4. *Nature*, **227**, 680–685.

LeBeau,J.M., Tedeschi B and Walter,G. (1991) Increased expression of pp60c-Src protein-tyrosine kinase during peripheral nerve regeneration. *Neurosci. Res.*, **28**, 299–309.

Lev,S., Moreno,H., Martinez,R., Canoll,P., Peles,E., Musacchio,J.M., Plowman,G.D., Rudy,B. and Schlessinger,J. (1995) Protein tyrosine kinase PYK2 involved in Ca^{2+}-induced regulation of ion channel and MAP kinase functions. *Nature*, **376**, 737–745.

Maletic-Savatic,M., Lenn,N.J. and Trimmer,J.S. (1995) Differential spatiotemporal expression of K^+ channel polypeptides in rat hippocampal neurons developing *in situ* and *in vitro*. *J. Neurosci.*, **15**, 3840–3851.

Mi,H., Deerink,T.J., Ellisman,M. and Schwarz,T.L. (1995) Differential distribution of closely related potassium channels in rat Schwann cells. *J. Neurosci.*, **15**, 3761–3774.

Migita,K., Eguchi,K., Kawabe,Y. and Nagataki,S. (1995) Tyrosine phosphorylation participates in peripheral T-cell activation and programmed cell death. *Immunology*, **85**, 550–555.

Mirsky,R. and Jessen,K.R. (1996) Schwann cell development, differentiation and myelination. *Curr. Opin. Neurobiol.*, **6**, 89–96.

Moarefi,I., LaFevre-Bernt,M., Sicheri,F., Huse,M., Lee,C.-H., Kuriyan,J. and Miller,W.T. (1997) Activation of the Src family tyrosine kinase Hck by SH3 domain displacement. *Nature*, **385**, 650–653.

Pappas,C.A. and Ritchie,J.M. (1998) Effect of specific ion channel blockers on cultured Schwann cell proliferation. *Glia*, **22**, 113–120.

Pappas,C.A., Ullrich,N. and Sontheimer H. (1994) Reduction of glial proliferation by K^+ channel blockers is mediated by changes in pH_i. *Neuroreport*, **6**, 193–196.

Patel,A.J., Lazdunski,M. and Honore,E. (1997) Kv2.1/kv9.3, a novel ATP-dependent delayed-rectifier K^+ channel in oxygen-sensitive pulmonary artery myocytes. *EMBO J.*, **16**, 6615–6625.

Prevarskaya,N.B., Skryma,R.N., Vacher,P., Daniel,N., Djiane,J. and Dufy,B. (1995) Role of tyrosine phosphorylation in potassium channel activation. *J. Biol. Chem.*, **270**, 24292–24299.

Qian,D., Lev,S., van Oers,N.S., Dikic,I., Schlessinger,J. and Weiss,A. (1997) Tyrosine phosphorylation of Pyk2 is selectively regulated by Fyn during TCR signaling. *J. Exp. Med.*, **185**, 1253–1259.

Ritchie,J.M. (1992) Voltage-gated ion channels in Schwann cells and glia. *Trends Neurosci.*, **15**, 345–351.

Roche,S., Fumagalli,S. and Cortneidge,S.A. (1995) Requirement for Src family protein tyrosine kinases in G_2 for fibroblast cell division. *Science*, **269**, 1567–1569.

Ross,C.A., Wright,G.E., Resh,M.D., Pearson,C.A. and Snyder,S.H. (1988) Brain-specific Src family oncogene mRNA mapped in rat brain by *in situ* hybridization. *Proc. Natl Acad. Sci. USA*, **85**, 9831–9835.

Salinas,M., Duprat,F., Heurteaux,C., Hugnot,J.P. and Lazdunski,M. (1997a) New modulatory α subunits for mammalian *Shab* K+ channels. *J. Biol. Chem.*, **272**, 24371–24379.

Salinas,M., de Weille,J., Guillemare,E., Lazdunski,M. and Hugnot,J.P. (1997b) Modes of regulation of Shab K^+ channel activity by the Kv8.1 subunit. *J. Biol. Chem.*, **272**, 8774–8780.

Songyang,Z. *et al*. (1993) SH2 domains recognize specific phosphopeptide sequences. *Cell*, **72**, 767–778.

Songyang,Z. *et al*. (1995) Catalytic specificity of protein-tyrosine kinases is critical for selective signalling. *Nature*, **373**, 536–539.

Sontheimer,H. (1994) Voltage-dependent ion channels in glial cells. *Glia*, **11**, 156–172.

Sontheimer,H. (1995) Glial neuronal interactions: a physiological perspective. *Neuroscientist*, **1**, 328–337.

Stewart,H.J.S., Bradke,F. Tabernero,A., Morrell,D., Jessen,K.R. and Mirsky,R. (1996) Regulation of rat Schwann cell P_0 expression and DNA synthesis by insulin-like growth factors *in vitro*. *Eur. J. Neurosci.*, **8**, 553–564.

Swope,S.L. and Huganir,R.L. (1994) Binding of nicotinic acetylcholine receptor to SH2 domains of Fyn and fyk protein tyrosine kinases. *J. Biol. Chem.*, **269**, 29817–29824.

Syroid,D., Maycox,P., Burrola,P., Liu,N.,Wen, D and Lemke G. (1996) Cell death in the Schwann cell lineage and its regulation by neuregulin. *Proc. Natl Acad. Sci. USA*, **93**, 9229–9234.

Szabo,I., Gulbins,E., Apfel,H., Zhang,X., Barth,P., Busch,A.E., Schlottmann,K., Pongs,O. and Lang,F. (1996) Tyrosine phosphorylation-dependent suppression of a voltage-gated K^+ channel in T lymphocytes upon Fas stimulation. *J. Biol. Chem.*, **271**, 20465–20469.

Thomas,S.M. and Brugge,J.S. (1997) Cellular functions regulated by Src family kinases. *Ann. Rev. Cell. Dev. Biol.*, **13**, 513–609.

Trachtenberg,J.T. and Thompson,W.J. (1996) Schwann cell apoptosis at developing neuromuscular junctions is regulated by glial growth factor. *Nature*, **379**, 174–177.

Trotter,J., Boulter,C.A., Sontheimer,H., Schachner,M. and Wagner,E.F. (1989) Expression of v-Src arrests murine glial cell differentiation. *Oncogene*, **4**, 457–464.

Tsai,W., Morielli,A.D. and Peralta,E.G. (1997) The m1 muscarinic acetylcholine receptor transactivates the EGF receptor to modulate ion channel activity. *EMBO J.*, **16**, 4597–4605.

Uehara,Y. and Fukazawa,H. (1991) Use and selectivity of Herbimycin A as inhibitor of protein-tyrosine kinases. In Hunter,T. and Sefton,B.M. (eds), *Protein Phosphorylation*. Academic Press, San Diego, CA, pp. 370–378.

Umemori,H., Wanaka,A., Kato,H., Takeuchi,M., Tohyama,M. and Yamamoto,T. (1992) Specific expressions of Fyn and Lyn, lymphocyte antigen receptor-associated tyrosine kinases, in the central nervous system. *Mol. Brain Res.*, **16**, 303–310.

Umemori,H., Sato,S., Yagi,T., Aizawa,S. and Yamamoto,T. (1994) Initial events of myelination involve Fyn tyrosine kinase signalling. *Nature*, **367**, 572–576.

Wilson,G.F. and Chiu,S.Y. (1990) Potassium channel regulation in Schwann cells during early developmental myelinogenesis. *J. Neurosci.*, **10**, 1615–1625.

Wilson,G.F. and Chiu,S.Y. (1993) Mitogenic factors regulate ionic channels in Schwann cells cultured from newborn rat sciatic nerve. *J. Physiol.*, **470**, 501–520.

Yu,S.P. *et al*. (1997) Mediation of neuronal apoptosis by enhancement of outward potassium current. *Science*, **278**, 114–117.

Yu,X.-M., Askalan,R., Keil II,G.J. and Salter,M.W. (1997) NMDA channel regulation by channel-associated protein tyrosine kinase Src. *Science*, **275**, 674–678.

Zorick,T.S. and Lemke,G. (1996) Schwann cell differentiation. *Curr. Opin. Cell. Biol.*, **8**, 870–876.

Received May 15, 1998; revised and accepted June 17, 1998